Polymer 51 (2010) 4735–4743

Contents lists available at ScienceDirect

Polymer

journal homepage: www.elsevier.com/locate/polymer

Metallocene-catalyzed synthesis of polyethylenes with side-chain triarylamines: Effects of catalyst structure and triarylamine functionality

Myung Hwan Park [a,1], Jun Ha Park [a,1], Youngkyu Do [a,**], Min Hyung Lee [b,*]

[a] Department of Chemistry, KAIST, Daejeon 305-701, Republic of Korea
[b] Department of Chemistry and Energy Harvest-Storage Research Center, University of Ulsan, Ulsan 680-749, Republic of Korea

ARTICLE INFO

Article history:
Received 29 June 2010
Received in revised form
13 August 2010
Accepted 14 August 2010
Available online 21 August 2010

Keywords:
Metallocene catalysts
Polyethylene
Triarylamine

ABSTRACT

The copolymerization of ethylene with 8-triarylamine (TAA) substituted 1-octene monomers (TAA = triphenylamine (**M1**), *N*,*N*-diphenyl-*m*-tolylamine (**M2**), *N*,*N*-diphenyl-1-naphthylamine (**M3**)) using various types of group 4 single-site catalytic systems (Cp_2ZrCl_2 (**C1**), *rac*-$EBIZrCl_2$ (**C2**), *rac*-$SBIZrCl_2$ (**C3**), *i*-$PrCpFluZrCl_2$ (**C4**), $Me_2Si(\eta^5\text{-}C_5Me_4)(\eta^1\text{-}N\text{-}^tBu)TiCl_2$ (**C5**)) was investigated to prepare functionalized polyethylene with side-chain TAA groups. The metallocene/methylaluminoxane (MAO) catalytic systems (**C1**–**C4**) efficiently lead to the production of high-molecular-weight poly(ethylene-*co*-**M1**). While the **C4**/MAO catalytic system shows the highest comonomer response, the **C5**/MAO system exhibits the poor compatibility with the **M1** comonomer. Copolymerization results of ethylene with **M1**–**M3** using **C4**/MAO indicate that **M1**–**M3** are well tolerated by both the cationic active species of **C4** and MAO cocatalyst, giving rise to the copolymers with high levels of activity and molecular weight. Inspection of the aliphatic region of the ^{13}C NMR spectra of the copolymers (**P1**–**P3**) having *ca.* 11 mol% of **M1**–**M3**, respectively, reveals the presence of isolated comonomer units with prevailing [EE**M**EE] monomer sequences in the polymer chain. UV–vis absorption and PL spectra exhibit an apparent low-energy band broadening for **P1** and **P2** indicative of intrachain aggregate formation. Whereas **P2** and **P3** undergo completely reversible one-electron oxidation process, **P1** shows relatively poor oxidational stability.

1. Introduction

Functionalized polyolefins have attracted great interest in a wide range of polyolefin applications since they can endow polyolefins with improved properties such as adhesion, dyeability, paintability, and compatibility with polar substrates. In addition to the chemical or free-radical modification of preformed polyolefins [1,2], a direct copolymerization of a functionalized olefin monomer using group 4 single-site catalytic systems has also proven to be a viable approach although the compatibility of a catalytic system with Lewis basic monomers is required for high catalyst performance [3–11]. Among the various functionalized polyolefins, amine-functionalized polyolefins may be particularly intriguing due to their applicability. For example, polyolefins with hindered aliphatic amines are reported to be effective light stabilizer of polyolefins [5,9]. It was also suggested that the end-functionalized polyolefins with amine groups could be useful for lubricant applications [12]. Recently, arylamine-functionalized polyolefins find their potential use as hole-transporting layer (HTL) materials in the optoelectronic device applications such as organic light-emitting diodes (OLEDs) due to their facile formation of stable radical cation of triarylamine, a proper HOMO level, and high thermal stability [3,6,13–18]. Since polyolefins generally possess excellent physical/mechanical properties as well as high chemical and thermal stability [19], the use of triarylamine (TAA)-functionalized polyolefin as HTL materials may be highly desired for the improvements in solution processability which is suitable for the fabrication of large-area and flexible OLEDs based on spin-coating and inkjet printing [20,21]. It was also previously demonstrated that the nonpolar polymer backbone is advantageous for the retention of hole mobility of the attached hole-transporting groups [22,23].

Regarding the optoelectronic device application, our group recently demonstrated that polyethylenes with pendant triphenylamine (TPA) groups can be efficiently produced by copolymerization of ethylene with 8-TPA substituted 1-octene monomer using *rac*-$Et(Ind)_2ZrCl_2$/MAO catalytic system and moreover such polymers can function as HTL materials in OLEDs [13]. It was also

* Corresponding author. Tel.: +82 52 259 2335; fax: +82 52 259 2348.
** Corresponding author. Tel.: +82 42 350 2829; fax: +82 42 350 2810.
E-mail addresses: ykdo@kaist.ac.kr (Y. Do), lmh74@ulsan.ac.kr (M.H. Lee).
[1] Tel.: +82 42 350 2869; fax: +82 42 350 2810.

0032-3861/$ – see front matter © 2010 Elsevier Ltd. All rights reserved.
doi:10.1016/j.polymer.2010.08.033

found that the polymerization behavior such as catalytic activity and comonomer enchainment is largely affected by the steric bulkiness of TPA moiety rather than possible Lewis acid–base interactions between cationic active species and triarylamine groups. Taking into account that the single-site catalytic systems can lead to the tailored polymer architecture via a highly controlled manner in terms of molecular weight, functionalities, and degree of incorporation of functional groups from varying the catalyst structure [2,24–26], a proper choice of the catalytic system may provide an efficient route to control the amount of TAA moieties in the polymer chain, as well as to investigate the occurrence of Lewis acid–base interactions between cationic active species and triarylamine groups that would detrimentally affect catalyst performance. Furthermore, since the properties of polymers are primarily related to the pendant triarylamine functionality, the variation of side-chain TAA group could also be useful in attaining novel polymer properties.

In a continuous effort to this area [13,27], the various kinds of group 4 single-site catalysts were examined to optimize the copolymerization reactions of ethylene with TAA-containing α-olefin monomers, which would thus allow for the efficient preparation of the TAA-functionalized polyethylene. The selected catalyst was further investigated to produce the polyethylenes bearing different TAA functionality. Details of synthesis and characterization of polymers are described in this contribution.

2. Experimental

2.1. Materials

All operations were performed under an inert nitrogen atmosphere using standard Schlenk and glove box techniques. Anhydrous grade solvents (Aldrich) were dried by passing through an activated alumina column and stored over activated molecular sieves (5 Å). Commercial reagents were used without any further purification after purchasing from Aldrich (4-Bromotriphenylamine, *t*-BuLi (1.7 M solution in *n*-pentanes), 1-octene, triphenylamine (TPA)) and Strem (zirconocene dichloride (Cp_2ZrCl_2, **C1**), *rac*-ethylenebis (indenyl)zirconium dichloride (*rac*-$EBIZrCl_2$, **C2**), *rac*-dimethylsilylbis(indenyl)zirconium dichloride (*rac*-$SBIZrCl_2$, **C3**)). Isopropylidene(cyclopentadienyl)(fluorenyl)zirconium dichloride (*i*-$PrCpFluZrCl_2$, **C4**) [28], dimethylsilyl(tetramethylcyclopentadienyl)(*tert*-butylamido)titanium dichloride ($Me_2Si(\eta^5\text{-}C_5Me_4)(\eta^1\text{-}N\text{-}^tBu)TiCl_2$, **C5**) [29–31], 8-bromo-1-octene [32], *N*-(4-bromophenyl) phenyl-*m*-tolylamine [33], *N*-(4-bromophenyl)-1-naphthylphenylamine [34], and 4-(7-octen-1-yl)-*N*,*N*-diphenylaniline (**M1**) [13] were synthesized by the published procedures. 1,1,2,2-Tetrachloroethane (TCE) was used as received from TCI. Polymerization-grade ethylene monomer from Honam Petrochemical Co. was used after purification by passing through Labclear™ and Oxiclear™ filters. 1-Octene was dried by passing through an activated alumina column. Methylaluminoxane (MAO) was used as a solid MAO obtained by evaporation of the solvent from a toluene solution of PMAO (Chemtura, 30 T). $CDCl_3$ and 1,1,2,2,-tetrachloroethane-d_2 ($C_2D_2Cl_4$) from Cambridge Isotope Laboratories were used after drying over activated molecular sieves (5 Å).

2.2. Measurements

NMR spectra of compounds were recorded on a Bruker Avance 400 spectrometer (400.13 MHz for ^1H, 100.62 MHz for ^{13}C) at ambient temperature. Chemical shifts are given in ppm, and are referenced against external Me_4Si (^1H, ^{13}C). HR EI-MS measurement (JEOL JMS700) was carried out at Korea Basic Science Institute (Daegu). UV–vis and PL spectra were recorded on a Jasco V-530 and a Spex Fluorog-3 Luminescence spectrophotometer, respectively, in TCE solvent with a 1-cm quartz cuvette. Cyclic voltammetry experiment was performed using an AUTOLAB/PGSTAT12 system.

2.3. Synthesis of monomers, *M2* and *M3*

An analogous method for **M1** [13] was employed using *N*-(4-bromophenyl)arylphenylamine (aryl = *m*-tolyl for **M2** and 1-naphthyl for **M3**) as a starting material. A solution of *N*-(4-bromophenyl)arylphenylamine (30.6 mmol) in THF (50 mL) was treated with 2 equiv of *t*-BuLi (36.0 mL) at −78 °C. After stirring for 1 h, the reaction mixture was allowed to warm to room temperature and stirred briefly at this temperature. The reaction vessel was cooled to 0 °C and the solution of 8-bromo-1-octene (6.30 g, 33.0 mmol) in THF (50 mL) was added dropwise into the cooled solution. The reaction mixture was slowly allowed to warm to room temperature and stirred overnight. The resulting solution was treated with 50 mL of a saturated aqueous solution of NH_4Cl and the organic portion was separated. The aqueous layer was further extracted with diethyl ether (2 × 30 mL). The combined organic portions were dried over $MgSO_4$, filtered, and evaporated to dryness. The dark oily crude product was sequentially purified by flash column chromatography on silica (eluent: *n*-hexane) and vacuum sublimation to remove unreacted 8-bromo-1-octene and triarylamine side product, respectively, affording the monomers as pale yellow oil. 4-(7-Octen-1-yl)-*N*-phenyl-*N*-*m*-tolylaniline (**M2**): Yield = 10.4 g (92%). ^1H NMR ($CDCl_3$) [ppm] δ 1.37 (m, 6H, 3,4,5-CH_2), 1.63 (m, 2H, 2-CH_2), 2.05 (m, 2H, 6-CH_2), 2.25 (s, 3H, 9-CH_3), 2.57 (t, J = 7.8 Hz, 2H, 1-CH_2), 4.95 (dd, J = 10.2/1.6 Hz, 1H, CH_2=CH), 5.01 (dd, J = 17.2/1.6 Hz, 1H, CH_2=CH), 5.82 (ddt, J = 17.2/10.2/6.6 Hz, 1H, CH_2=CH), 6.80 (d, J = 7.4 Hz, 1H), 6.87 (d, J = 8.0 Hz, 1H), 6.92–6.97 (m, 2H), 6.99–7.13 (m, 7H), 7.20 (t, J = 8.0 Hz, 2H). ^{13}C NMR ($CDCl_3$) [ppm] δ 21.39 (9-CH_3), 28.82, 28.95, 29.18 (3,4,5-CH_2), 31.40 (2-CH_2), 33.74 (6-CH_2), 35.32 (1-CH_2), 114.20 (CH_2=CH), 121.09, 122.01, 123.25, 123.55, 124.48, 124.55, 128.90, 129.00, 129.06, 137.41, 138.83, 139.01 (CH_2=CH), 145.44, 147.92, 148.11. HR EI-MS: m/z calcd for $C_{27}H_{31}N$, 369.2457; found, 369.2459.

4-(7-Octen-1-yl)-*N*-1-naphthyl-*N*-phenylaniline (**M3**): Yield = 11.2 g (90%). ^1H NMR ($CDCl_3$) [ppm] δ 1.38 (m, 6H, 3,4,5-CH_2), 1.62 (m, 2H, 2-CH_2), 2.07 (m, 2H, 6-CH_2), 2.56 (t, J = 7.8 Hz, 2H, 1-CH_2), 4.97 (dd, J = 10.2/1.6 Hz, 1H, CH_2=CH), 5.03 (dd, J = 17.0/1.6 Hz, 1H, CH_2=CH), 5.84 (ddt, J = 17.0/10.2/6.7 Hz, 1H, CH_2=CH), 6.91 (t, J = 7.3 Hz, 1H), 6.99–7.08 (m, 6H), 7.17–7.21 (m, 2H), 7.33–7.38 (m, 2H), 7.44–7.49 (m, 2H), 7.77 (d, J = 8.0 Hz, 1H), 7.89 (d, J = 8.2 Hz, 1H), 7.99 (d, J = 8.4 Hz, 1H). ^{13}C NMR ($CDCl_3$) [ppm] δ 28.83, 28.96, 29.16 (3,4,5-CH_2), 31.42 (2-CH_2), 33.76 (6-CH_2), 35.24 (1-CH_2), 114.16 (CH_2=CH), 120.93, 120.99, 121.81, 122.48, 124.35, 126.02, 126.18, 126.23, 126.31, 127.06, 128.30, 128.94, 128.98, 129.05, 131.27, 135.24, 136.61, 139.12 (CH_2=CH), 143.76, 146.02, 148.79. HR EI-MS: m/z calcd for $C_{30}H_{31}N$, 405.2457; found, 405.2459.

2.4. Polymerization procedure

Into the 250 mL-glass reactor charged with a pre-weighed MAO ([Al]/[Cat.] = 1000 or 2000) was transferred a toluene solution of a prescribed amount of comonomer (49.5 mL), and the temperature was adjusted to 75 °C using an external bath. Ethylene monomer was then saturated at 1 bar with vigorous stirring for 10 min after degassing several times. Polymerization was started by the injection of a toluene solution of catalyst (0.5 mL, 1.0 μmol of catalyst). The polymerization time was varied to keep the comonomer conversion low (typically below 20%). The reactions were quenched by the injection of *ca.* 2 mL of 10% HCl solution of EtOH. The resultant mixture was then poured into the large volume of acidified EtOH (2%, 500 mL) and stirred for 1 h. The precipitated polymer

was subsequently collected by filtration and washed with EtOH (3 × 50 mL). The resulting polymers were finally dried in a vacuum oven at 70 °C to constant weight.

2.5. Polymer analysis

^{1}H NMR spectra of the polymers were recorded on a Bruker Avance 400 spectrometer at 100 °C. ^{13}C NMR spectra were obtained from a Bruker AMAX 500 (^{13}C; 125.77 MHz) spectrometer at 120 °C with 90° pulse angle, 2 s acquisition time, and 8 s relaxation delay. The samples were dissolved in $C_2D_2Cl_4$ (for ^{1}H, *ca.* 5 mg and for ^{13}C, *ca.* 90 mg in 0.5 mL) in 5-mm tubes. All the measurements were performed after complete dissolution by pre-heating the samples to about 110 °C in an oil bath. The comonomer contents in the polymers were determined from ^{1}H NMR spectra. ^{13}C NMR peak assignments of the polymers in the aliphatic region were analogously made according to the reported literatures [35,36]. The molecular weight (M_n and M_w) and polydispersity (M_w/M_n) of the polymers were analyzed by high temperature gel-permeation chromatography (GPC) on a Polymer Laboratories PL 220 at 140 °C in 1,2,4-trichlorobenzene and calibrated using narrow polystyrene standards as a reference. The melting transition and glass transition temperatures (T_m and T_g) of the polymers were measured by differential scanning calorimetry (DSC, TA Instrument Q100) at a heating rate of 10 °C/min. Any thermal history in the polymers was eliminated by first heating the samples to 180 °C, cooling to −70 °C at 20 °C/min, and then recording the second DSC scan from −70 °C to 180 °C at 10 °C/min. Thermogravimetric analyses (TGA) were performed under N_2 atmosphere using a TA Instrument Q500 at a heating rate of 20 °C/min from 50 °C to 800 °C.

2.6. UV–vis absorption and photoluminescence measurements

Due to high toxicity of TCE solvent, great caution should be exercised when handling and preparing solutions. UV–visible absorption and PL measurements were performed in TCE solvent with a 1-cm quartz cuvette at ambient temperature. The TCE solvent was used after purification by distillation. The polymer used for the measurements was purified by precipitation from a TCE solution into EtOH. The samples were first dissolved in hot TCE and then diluted to the desired concentrations based on triarylamine groups at ambient temperature. Quinine sulfate was used as the standard for determination of the quantum yields (1×10^{-4} M in 0.5 M H_2SO_4, $\Phi_F = 0.55$) [37].

2.7. Cyclic voltammetry

Cyclic voltammetry measurements were carried out with a three-electrode cell configuration consisting of platinum working and counter electrodes and a $Ag/AgNO_3$ (0.1 M in acetonitrile) reference electrode at room temperature. The coated polymer on the platinum wire was used as the sample. The solvent was acetonitrile and 0.1 M tetrabutylammonium hexafluorophosphate was used as the supporting electrolyte. The oxidation potentials were recorded at a scan rate of 50 mV/s and reported with reference to the ferrocene/ferrocenium (Fc/Fc^+) redox couple.

3. Results and discussion

3.1. Catalyst screening

It is highly desirable for catalyst to be able to readily produce copolymer having a high content of TAA moieties for the facile control of hole-transporting properties. Although the sterically open catalyst structure would be definitely advantageous for controlling the level of incorporation of large comonomer such as TAA-containing α-olefin monomer and thereby leading to the copolymer of a controlled amount of TAA moieties, it was found in the previous reports that the incorporation of comonomer into the polyethylene backbone may be inhibited by not only steric effect of comonomer, but also Lewis acid–base interactions between the cationic active species of catalyst and the amine functionalities [5,7,13]. Since the steric openness of catalyst structure and the extent of such Lewis acid–base interactions are expected to correlate positively with each other, both factors should be considered together in the catalyst selection. Thus, the copolymerization reactions between ethylene and TPA-containing α-olefin monomer using various types of catalyst structures having different steric openness at the metal center were first investigated to choose an optimal catalyst for the efficient copolymerization.

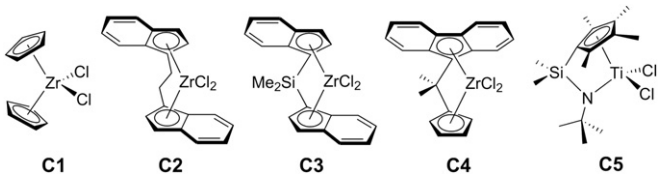

Chart 1.

Among the single-site catalysts developed so far, the well-known catalyst structures including the previously examined *rac*-Et$(Ind)_2ZrCl_2$ (**C2**) were employed as catalyst (Chart 1). It is well established in the copolymerization of ethylene or propylene with higher α-olefins that the ability to incorporate α-olefins is in the increasing order from **C1** to **C5** [38,39], which is closely related to their steric openness at the metal center [40]. 4-(7-Octen-1-yl)-*N*,*N*-diphenylaniline monomer (**M1**) was introduced as a comonomer.

The copolymerization reactions of ethylene and **M1** were achieved at 75 °C under atmospheric ethylene pressure upon MAO activation (Scheme 1). As can be seen in Table 1, all the catalytic systems efficiently lead to the production of the copolymer (**P1**) with a decreasing tendency of activity [(kg polymer)/((mol of cat.)·h·bar)] from **C1** to **C5** (runs 1–5) although **C1** and **C2** show a similar level of activity. The decrease of activity is most apparent for the **C5** catalytic system. GPC results indicate the formation of high-molecular-weight copolymers from *ansa*-type catalysts (**C2**–**C5**), but the non-bridged **C1** shows low molecular weight.

The unimodal and narrow molecular weight distribution with a polydispersity of *ca.* 2 indicates the involvement of single active species in the copolymerization. Estimation of the comonomer content from the ^{1}H NMR spectra reveals that the comonomer **M1** is readily incorporated into the polyethylene backbone and the extent of the incorporation increases upon varying the catalyst structure from **C1** to **C5** at the given comonomer concentration.

While the decreasing melting transition (T_m) of the copolymers correlates very well with the increasing content of **M1**, the additional weak high-melting peak at 119 °C is unexpectedly observed for the copolymer from the **C5** catalytic system (run 5) as evidenced

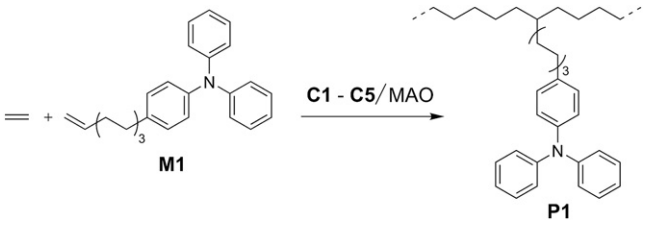

Scheme 1. Synthesis of **P1** with **C1**–**C5**/MAO catalysts.

Table 1
Copolymerization results of ethylene and **M1** with **C1**–**C5**/MAO.[a]

Run	Cat.	[**M1**] (M)	[**TPA**]/[Cat.]	T_p (sec)	Yield (g)	Activity[d]	$10^{-3}M_w$[e]	M_w/M_n[e]	Content of **M1**[f] (mol %)	T_m[g] (°C)	T_{d5}[h] (°C)
1	**C1**	0.0563	2815	43	0.353	29.5×10^3	43	21.9	0.9	123.8	447
2	**C2**	0.0563	2815	45	0.377	30.2×10^3	119	2.17	1.8	115.2	451
3	**C3**	0.0563	2815	42	0.266	22.8×10^3	177	2.57	2.4	109.5	450
4	**C4**	0.0563	2815	60	0.166	10.0×10^3	136	1.92	4.0	100.5	446
5	**C5**	0.0563	2815	780	0.368	1.7×10^3	179	1.72	6.8	82.6/118.5	431
6	**C4**	0.113	5650	150	0.300	7.2×10^3	143	1.74	7.8	81.1	442
7	**C4**	0.169	8450	600	0.920	5.5×10^3	118	2.33	11.6	n/o[i]	442
8	**C5**	0.113	5650	1020	0.092	0.3×10^3	333	2.29	5.4	111.7/127.7	n/d[j]
9[b]	**C4**	0.0563	0	60	0.230	13.8×10^3			8.8	n/o[i]	n/d
10[b,c]	**C4**	0.0563	2815	60	0.190	11.4×10^3			8.4	79.7	n/d

[a] Conditions: [Cat.] = 1.0 μmol; MAO = methylaluminoxane; P_E = 1 bar; [Al]/[Cat.] = 1000; T_p = 75 °C; solvent = 50 mL of toluene.
[b] 1-Octene comonomer.
[c] In the presence of molecular triphenylamine (TPA).
[d] Activity given in units of (kg polymer)/((mol of cat.)·h·bar).
[e] Determined by GPC.
[f] Determined by ^{1}H NMR.
[g] Determined by DSC.
[h] Determined by TGA at 5% weight loss.
[i] Not observed.
[j] Not determined.

from the DSC trace in Fig. 1. This result may indicate that the copolymers from **C5** consist of a mixture of polymers with different lengths of ethylene sequence.

To elucidate this feature, the copolymerization using the **C5** catalytic system was examined at the higher **M1** concentration in the feed (run 8). Remarkably, the result shows not only the sharp decrease of catalytic activity, but also the reduced comonomer incorporation when compared to that obtained at the lower **M1** concentration. Inspection of the DSC curve further reveals the appearance of two high-melting peaks without any indication of the formation of the copolymer corresponding to the expected comonomer content, thus indicating that the comonomer **M1** is poorly compatible with the cationic active species of **C5** in the copolymerization in terms of both activity and comonomer incorporation. This finding suggests that the large steric openness at the metal center of **C5** allows the strong Lewis acid–base interactions between the cationic metal center and the TPA group in **M1**, leading to inhibition of the monomer insertion, particularly the sterically bulky **M1** comonomer and thereby giving rise to the formation of polymer chains with longer ethylene sequences.

To gain insights into the copolymerization reactions of other metallocene systems (**C1**–**C4**), control experiments of 1-octene copolymerization were investigated using the highly incorporating **C4** catalytic system in the presence and absence of molecular TPA. According to the results, the **C4** catalytic system shows both the slightly decreased activity and 1-octene incorporation in the presence of TPA (run 9 vs run 10), indicating that TPA interferes with the monomer insertions at the cationic active center of **C4** via Lewis acid–base interactions. In fact, this result is in parallel with the previous observation in the **C2** catalytic system [13]. Nonetheless, the retention of high level of activity and 1-octene incorporation in the presence of TPA may imply that the comonomer **M1** should be electronically well tolerated by the cationic active species of **C4** as shown from the high activity (run 4). To confirm the compatibility of the **C4** catalytic system with the **M1** comonomer, the copolymerization reactions at the increased concentration of **M1** in the feed were examined (runs 6 and 7). The results show the high level of activity with the moderate decrease upon increasing the concentration of **M1**. Particularly, the incorporation of **M1** increases nearly in proportion to the concentration of **M1** in the feed. In agreement with this observation, the relatively high reactivity ratio of **M1** in the **C4** catalyst ($r_{\mathbf{M1}} \approx 0.09$ and $r_E \approx 19.6$) in comparison with the previously calculated value in the **C2** catalyst ($r_{\mathbf{M1}} \approx 0$ and $r_E \approx 43$) [13] was estimated from curve fitting of the composition of the monomer feed to the copolymer compositions (runs 4, 6, 7 in Table 1) using the copolymerization equation based on the first-order Markov model [13,38] DSC and GPC results are also well consistent with the formation of uniform copolymers through single active species. All these results support the

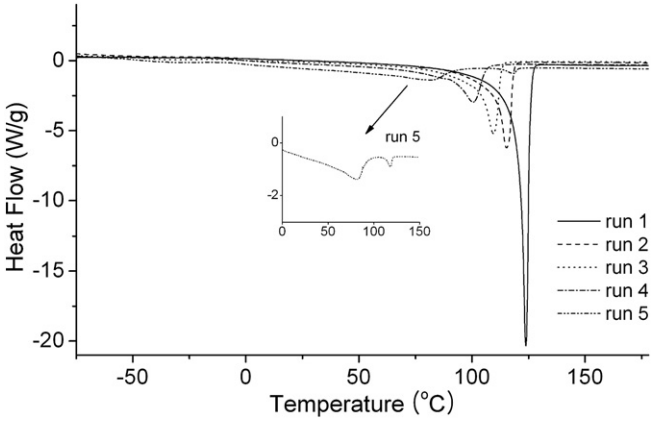

Fig. 1. DSC traces of **P1**s from **C1**–**C5** in Table 1.

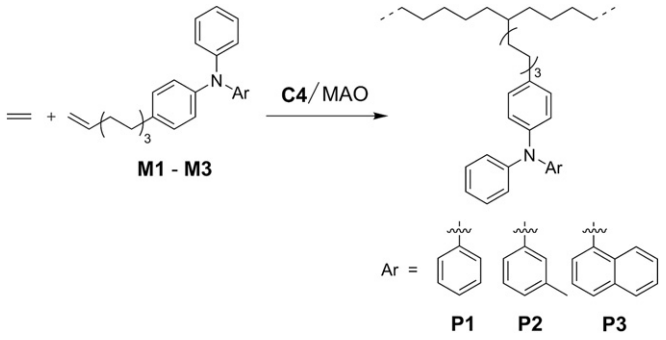

Scheme 2. Synthesis of **P1**–**P3** with **C4**/MAO catalyst.

Table 2
Copolymerization results of ethylene and **M1**–**M3** with **C4**/MAO.[a]

Run	Comon.	[Comon.] (M)	[**TAA**]/[Cat.]	T_p (sec)	Yield (g)	Activity[d]	$10^{-3}M_w$[e]	M_w/M_n[e]	Content of **M1**[f] (mol %)	T_m/T_g[g] (°C)	T_{d5}[h] (°C)
1[b]	**M1**	0.0563	2815	60	0.166	10.0×10^3	136	1.92	4.0	100.5	445
2	**M2**	0.0563	2815	60	0.350	21.0×10^3	164	2.48	5.1	92.5	449
3	**M3**	0.0563	2815	60	0.240	14.4×10^3	163	1.94	3.5	103.7	438
4[c]	**M1**	0.158	7900	300	0.470	5.6×10^3	92	1.74	11.4	n.o.[i]/−6.1	441
5[c]	**M2**	0.168	8400	390	1.075	9.9×10^3	122	1.83	12.6	n.o./−7.3	443
6[c]	**M3**	0.173	8650	450	0.880	7.0×10^3	123	1.51	11.3	n.o./9.9	445

[a] Conditions: [**C4**] = 1.0 μmol; MAO = methylaluminoxane; P_E = 1 bar; [Al]/[**C4**] = 1000; T_p = 75 °C; solvent = 50 mL of toluene.
[b] Data taken from run 4 in Table 1.
[c] [Al]/[**C4**] = 2000.
[d] Activity given in units of (kg polymer)/((mol of cat.) h bar).
[e] Determined by GPC.
[f] Determined by ^{1}H NMR.
[g] Determined by DSC.
[h] Determined by TGA at 5% weight loss.
[i] Not observed.

compatibility of the **C4** catalytic system with the **M1** comonomer. These findings thus suggest that the copolymerization reactions by the metallocene structures (**C1**–**C4**) are less significantly affected by the large degree of nitrogen functionality of the TPA groups probably owing to the steric protection of the metal center by both cyclopentadienyl ring fragments. In other words, it can be said that the degree of incorporation of **M1** is primarily governed by the steric openness at the metal center of the metallocene-type catalysts. From these preliminary studies, the **C4** catalytic system which shows the highest comonomer response was employed in the subsequent copolymerization reactions of ethylene with various TAA-containing α-olefin monomers.

3.2. Synthesis of polyethylenes with pendant triarylamines

The 8-TAA substituted 1-octene monomers (**M1**–**M3**) with different triarylamine moieties were considered as the TAA-containing α-olefin monomers. As the TAA moieties, the monoamine analogues of the well-known molecular HTL materials, TPD (4,4′-bis(phenyl-*m*-tolylamino)biphenyl) [41] and NPB (4,4′-bis(1-naphthylphenylamino)biphenyl) [42] were introduced for **M2** and **M3**, respectively. The **M2** and **M3** monomers could also be obtained in high yield (>90%) from the analogous method employed in the preparation of **M1** [13]. The copolymerization reactions of ethylene and **M1**–**M3** were first achieved using the **C4** catalytic system under the conditions described in the catalyst screening experiments (Scheme 2).

According to the polymerization results in Table 2, the high-molecular-weight **P2** and **P3** copolymers are also readily produced with high activity (runs 2 and 3). Interestingly, the activities are higher than that of the **P1** copolymer and the activity for the copolymerization of **M2** is highest among them. Furthermore, the comonomer incorporation is also highest for the **P2** copolymer while that of the **P3** is lowest. These results may indicate that the

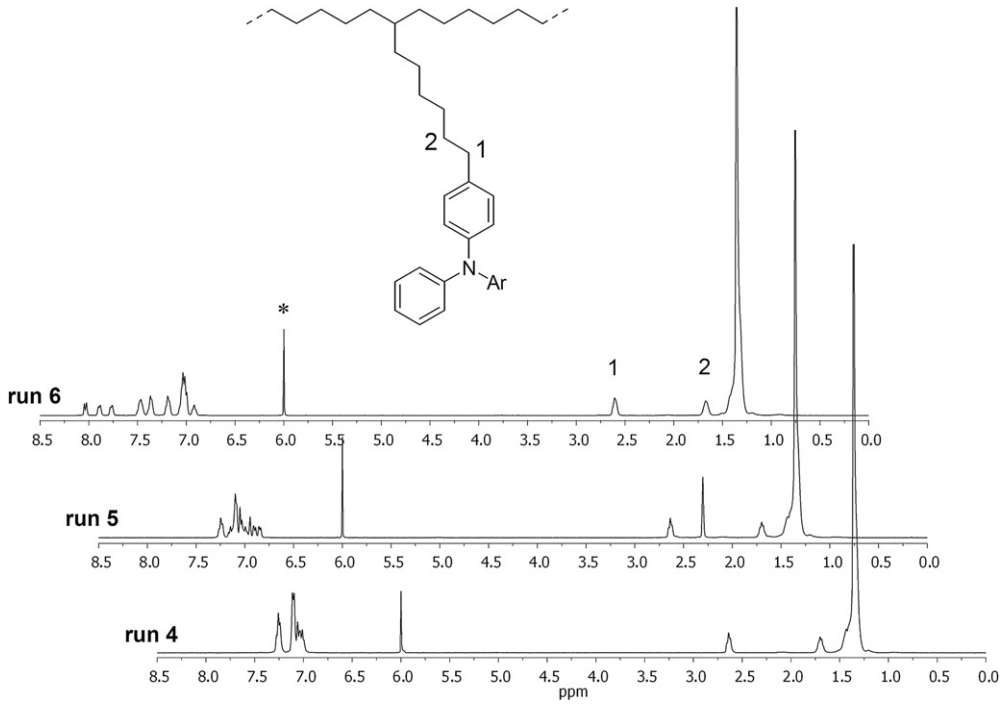

Fig. 2. ^{1}H NMR spectra of **P1**–**P3** from runs 4, 5 and 6, respectively, in Table 2 (*from $C_2D_2Cl_4$).

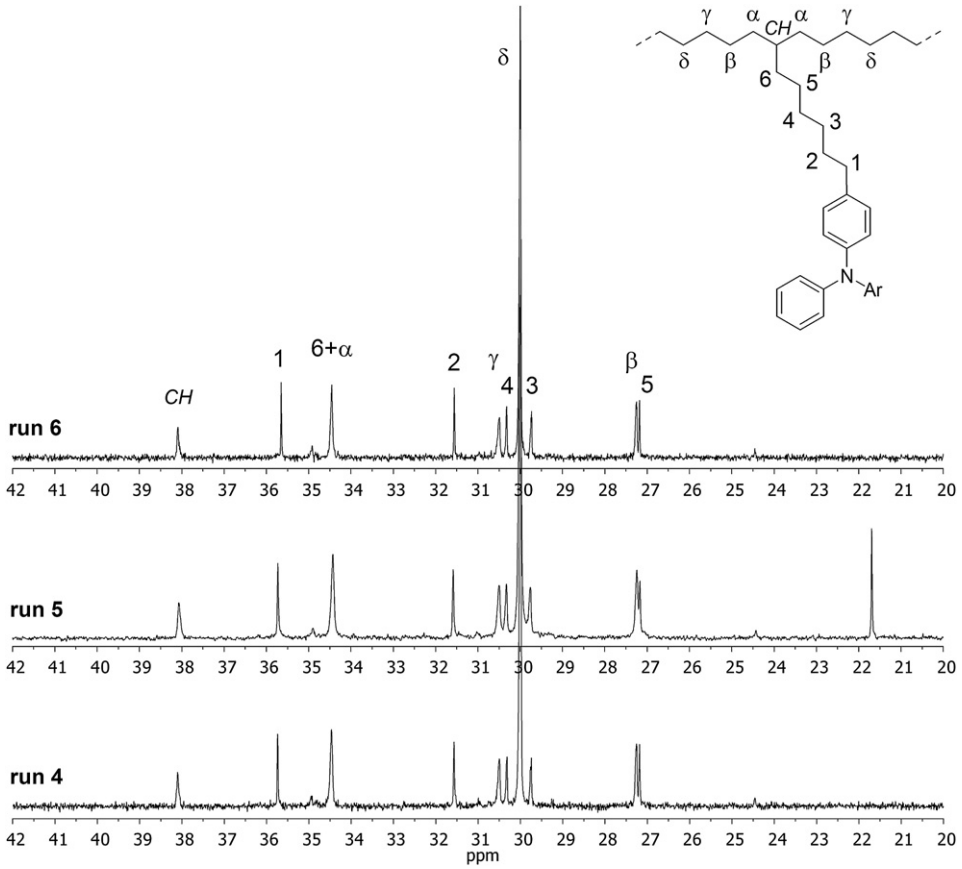

Fig. 3. An aliphatic region of ^{13}C NMR spectra of **P1**–**P3** from runs 4, 5 and 6, respectively, in Table 2. Peak assignments were made on the carbon resonances associated with the isolated comonomer units.

increase in the steric bulkiness of TAA group could lead to the reduction or prevention of Lewis acid–base interactions between the cationic metal center and the TAA group, rendering the copolymerization facile. The lower activity for the **M1** comonomer bearing the smallest TAA group than those for the **M2** and **M3** supports the involvement of such interactions in the copolymerization as similarly observed in the ethylene/1-octene copolymerizations in the presence of molecular TPA described above. Comparison of the polymerization results for **M2** and **M3** shows the dependence of the copolymerization on the steric effect of TAA group, suggesting that the nitrogen functionalities in both comonomers almost do not compete with the monomer insertions at the cationic metal center. The higher activity and comonomer incorporation observed for the **M2** copolymerization than those for the **M1** might be explained by the suggestion that the slight increase in steric bulkiness by the methyl substitution on the TAA group exert a negligible influence on the vinyl insertion probably due to the presence of a long carbon spacer between the vinyl and TAA groups while such an increase in steric bulkiness apparently reduce the extent of the direct Lewis acid–base interaction between the TAA group and the metal center. The narrow molecular weight distribution and single T_ms further indicate the formation of uniform copolymers, confirming that the **M2** and **M3** comonomers are well

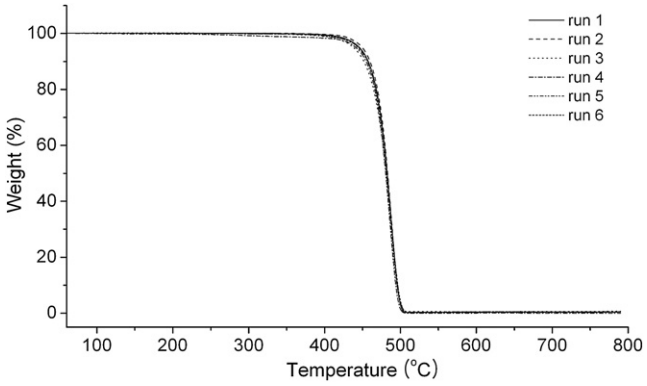

Fig. 4. TGA thermograms of **P1**–**P3** from runs 1–6 in Table 2.

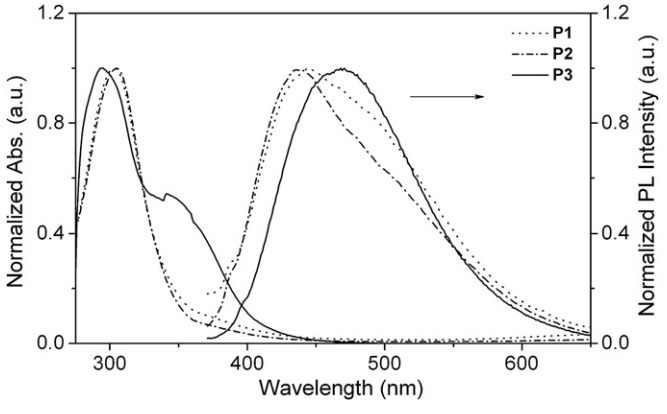

Fig. 5. UV–vis absorption (left) and PL (right) spectra of **P1**–**P3** from runs 4, 5 and 6 in Table 2.

Table 3
Optical and electrochemical data of **P1**–**P3**.

Polymer	λ_{abs}[a] (nm)	λ_{em} (Φ_F)[b] (nm)	E_g[c] (eV)	E_{ox} (V)	HOMO[f]/LUMO[g] (eV)
P1	303	444 (0.03)	3.48	0.601[d]	−5.44/−1.96
P2	303	438 (0.05)	3.47	0.564[e]	−5.39/−1.92
P3	294/342	468 (0.07)	3.08	0.568[e]	−5.40/−2.32

[a] Absorption measured in TCE (2.0×10^{-5} M based on TAA groups).
[b] Acquired using a 1.0×10^{-5} M solution. Quinine sulfate used as a standard ($\Phi_F = 0.55$).
[c] Estimated from the absorption edge.
[d] The oxidation onset potential vs a Fc/Fc^+ couple.
[e] Taken from the $E_{1/2}$ vs a Fc/Fc^+ couple.
[f] Calculated from the E_{ox}.
[g] Estimated from the HOMO and band gap (E_g) energies.

tolerated by both the cationic active species of **C4** and MAO cocatalyst.

Based on the forgoing copolymerization results, the copolymers having a moderate comonomer content were prepared for further consideration in the utilization as HTL materials. For comparison purpose, the copolymers having the similar comonomer content of *ca.* 11 mol% (±1 mol%) by ^{1}H NMR spectroscopy (*vide infra*) were prepared from the controlled polymerization reactions with the varied concentration of each comonomer in the feed (runs 4–6 in Table 2). Although the comonomer content was not optimized for the use in OLEDs, it is noted in the catalyst screening experiment that the copolymer having such comonomer content showed no apparent melting transition, pointing to the formation of an amorphous polymer (run 7 in Table 1). As similar to the **M1** copolymerization in Table 1, it can be seen that the copolymerization reactions at the large feed of the **M2** and **M3** comonomers also proceed in a well controlled manner, leading to the production of the **P2** and **P3** copolymers with high levels of activity and molecular weight. The identity of the copolymers was analyzed by ^{1}H and ^{13}C NMR spectroscopy and the spectra were shown in Figs. 2 and 3, respectively.

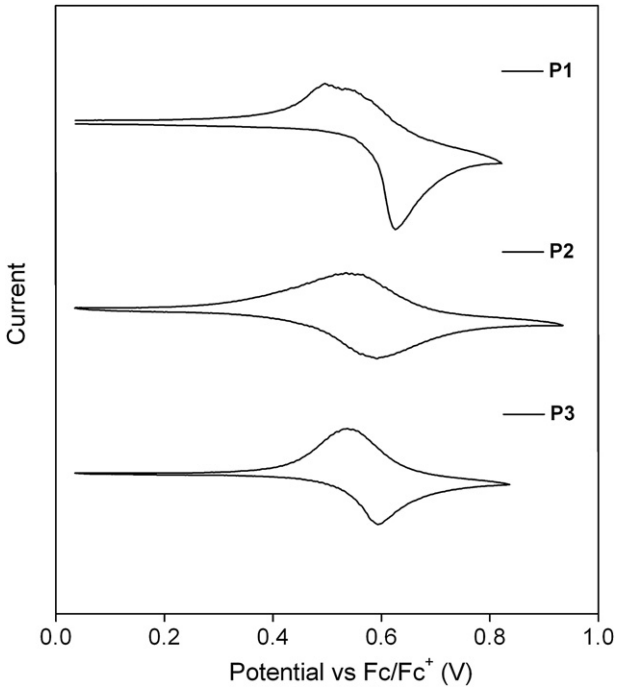

Fig. 6. Cyclic voltammograms of **P1**–**P3** measured at a scan rate of 50 mV/s in CH_3CN.

The ^{1}H NMR spectra of all the copolymers exhibit essentially identical resonances in the aliphatic region corresponding to the protons of the side-chain methylenes and the polyethylene backbone except for the additional methyl proton peak at δ 2.30 ppm for the tolyl moiety of **P2**. The aryl proton resonances are also well-differentiated between the TAA moieties. While the carbon resonances in the aromatic region of the ^{13}C NMR spectra indicate the existence of the TAA moieties in the copolymers, inspection of the aliphatic region of the ^{13}C NMR spectra reveals the well-resolved resonances from the side-chain and polyethylene backbone, as well as the isolated comonomer units in the polymer chains with the identical carbon resonance features for **P1**–**P3**. While the major carbon peaks attributable to the monomer sequence of [EE**M**EE] are clearly observed, there are no detectable carbon peaks associated with sequential comonomer incorporations corresponding to the [**MMM**] triad and [**MM**] dyads. Instead, the only observable are the very slight carbon peaks assignable to the [**M**E**M**] (δ 24.46 ppm, $\beta\beta$), [**M**EE**M**] (δ 30.97 ppm, $\gamma\gamma$), and [**M**E**M**E/E**M**E**M**] (δ 34.95 ppm, $\alpha\gamma$) sequences [35,36]. In spite of the moderate comonomer contents of *ca.* 11 mol%, these results are quite different from those found in the ethylene and usual α-olefin copolymerizations where the carbon peaks attributable to the sequential comonomer incorporations are apparently shown at such a comonomer content. This finding could be ascribed to the very low reactivity ratios of **M1**–**M3** comonomers, as similarly noted in the copolymerization of **M1** by **C2** catalyst [13]. Estimates for the comonomer content from the ^{13}C NMR spectra [36] are also in good agreement with those from the ^{1}H NMR spectra, only showing a slight difference within *ca.* 1 mol%. Overall, these results indicate that the copolymers constitute a well-defined structure.

While DSC measurements show no apparent melting transitions for **P1**–**P3** consistent with the increased comonomer incorporation, the glass transition is observed below an ambient temperature. Comparison of the T_g values for **P1**–**P3** indicates that the T_g of the naphthylamine-containing **P3** (9.9 °C) is higher than those of **P1** (−6.1 °C) and **P2** (−7.3 °C) whose values are very similar. Interestingly, this result is in parallel with the trend of T_gs found in the molecular triarylamine analogues for **P2** and **P3**, i.e. TPD (60–65 °C) and NPB (95–100 °C), respectively. This finding thus suggests that the pendant triarylamine moieties also contribute to the glass transition behavior of **P1**–**P3**. TGA measurements show high T_{d5} values ($T_{d5} > 441$ °C) for all the **P1**–**P3** (runs 4–6) comparable to those of the copolymers having a lower comonomer content (runs 1–3) and the 1-octene copolymers, indicating high thermal stability of the copolymers irrespective of the nature and the amount of TAAs (Fig. 4). Despite the poor solubility in common organic solvents, the copolymers showed good solubility in the chlorinated solvents such as 1,1,2,2,-tetrachloroethane (TCE) and chlorobenzene at elevated temperature.

3.3. Optical and electrochemical properties

The optical properties of the copolymers were examined by UV–vis and PL measurements in TCE. As shown in Fig. 5 and Table 3, **P1**–**P3** (runs 4–6 in Table 2) exhibit a major absorption band at 294–303 nm assignable to the π–π^* transitions in the triaylamine moieties. The additional low-energy absorption band observed for **P3** ($\lambda_{abs} = 342$ nm) could be ascribable to the transition to the lowest-lying π^* orbital localized on the naphthyl group [43]. The almost invariant absorption features for **P1** and **P2** indicate that methyl substitution at the phenyl ring of the triphenylamine moiety negligibly influences the electronic transition [44]. Although the absorption maximum wavelength for **P1** and **P2** is in good agreement with those observed for the copolymers having low **M1** contents reported previously [13], the weak low-energy

Table 4
Comparison of thermal, optical and electrochemical data of polyolefins with pendant triarylamines.

Entry	Polymer	**TAA**	T_g/T_{d5} (°C)	E_g (eV)	E_{ox} (V)	HOMO (eV)	LUMO (eV)	Ref.
1	**P1** (run 4)[a]	Ph_3N	−6.1/441	3.48	0.601[c]	−5.44	−1.96	this work
2	**P2** (run 5)[a]	Ph_2N(*m*-Tol)	−7.3/443	3.47	0.564[d]	−5.39	−1.92	this work
3	**P3** (run 6)[a]	Ph_2N(1-Naph)	9.9/445	3.08	0.568[d]	−5.40	−2.32	this work
4	**ENO5**	Ph_3N	n/d[b]	3.48	0.608[c]	−5.45	−1.97	[13]
5	**PNB Naph**	Ph_2N(1-Naph)	268/401	3.08	0.55[d]	−5.35	−2.27	[27]
6	**PNB NPB**	4,4′-[(1-Naph)PhN]$_2$Biph	365/449	3.00	0.31/0.53[d,e]	−5.11	−2.11	[27]

[a] In Table 2.
[b] Not determined.
[c] Quasi-reversible oxidation.
[d] Reversible oxidation.
[e] The second half-oxidation potential.

tails developed in the region between 350 and 450 nm might be suggestive of intrachain aggregate formation.

On the other hand, the emission spectra of **P1** and **P2** exhibit similar emission maximum wavelengths (λ_{em}) but the low-energy band broadening is apparently observed for both copolymers. It is noteworthy that such broadening was actually not observed for the copolymers having low **M1** contents up to 6.1 mol% and the λ_{em} of **P1** (444 nm) is also slightly red-shifted when compared to those of low-content copolymers ($\lambda_{em} = 436$ nm for 6.1 mol% of **M1**) [13]. As noted in the absorption spectra, these results could be attributed to the intrachain aggregation between the side-chain TAA groups promoted by the flexible nature of the polymer backbone and the increased amount of neighboring TAA groups [45]. Since the broadening of the emission band is more pronounced in **P1** and hardly observable for **P3**, such aggregation appears to be quite dependent upon the steric bulkiness of the TAA groups, as similarly found in the luminescent borane polymers [46]. The very low fluorescence quantum yields of the copolymers are also supportive of aggregate formation that may lead to emission quenching.

The electrochemical behavior of the copolymers was investigated by cyclic voltammetry (CV). According to the cyclic voltammograms shown in Fig. 6, it can be seen that **P1**–**P3** undergo one-electron oxidation process. In contrast to the completely reversible redox behavior observed for **P2** and **P3**, however, the oxidation wave of **P1** is not reversible as previously observed for the low-content **M1** copolymer [13]. This result indicates that the radical cations derived from **P2** and **P3** are stable due to the substitution at the phenyl ring which may prevent dimerization of triarylamine radicals to tetraarylbenzidine species after oxidation [47]. Finally, the HOMO and LUMO energy levels of **P1**–**P3** were calculated from the optical band gap (E_g) and oxidation onset potential (E_{ox}) measured by the UV–vis absorption and cyclic voltammetry, respectively, and are given with respect to zero vacuum level in Table 3 [48]. The HOMO and LUMO levels for **P1**–**P3** are calculated to be *ca.* −5.4 eV and −1.9 to −2.3 eV, respectively. These levels fall in the typical range observed for triarylamine-based HTL materials and thus is expected to show hole-transporting ability when incorporated into HTL of OLED devices.

3.4. Comparison of thermal, optical, and electrochemical properties of polyolefins with pendant triarylamines

In order to see the feasibility of **P1**–**P3** (runs 4–6 in Table 2) for the use as HTL materials in OLED devices, we compared the thermal, optical, and electrochemical properties of **P1**–**P3** with those of the relevant polyolefins with pendant TAAs reported previously [13,27]. The comparative data given in Table 4 indicate that while both the polymers based on polyethylene (entries 1–4) and polynorbornene backbone (entries 5–6) show similar high thermal stability from their high T_{d5} values (>400 °C), the low T_gs of polyethylene-based copolymers (entries 1–4) due to flexibility of polymer backbone might result in the lower long-term device stability than the devices based on the polynorbornene derivatives (entries 5–6). It can be seen that the optical and electrochemical properties of polymers are solely dependent upon TAA functionality. The high oxidation potentials which in turn lead to the deep HOMO levels for the TPA-containing polymers (entries 1 and 4) indicate the low stability of radical cations as shown from the quasi-reversibility of cyclic voltammograms. It is interesting to note that the content of TPA moiety in **P1** (11.4 mol%) and **ENO5** (6.1 mol %) [13] almost does not affect the oxidation potential and HOMO level, being consistent with the electronic isolation between the side-chain TAA groups in the copolymers. While the *m*-tolyl substituted **P2** shows a comparable band gap due to the identical electronic transition with that of **P1**, the lower oxidation potential (higher HOMO level) with a reversible oxidation feature may lead to better hole-transporting property than **P1**. On the other hand, the naphthyl substituted TAA polymers (entries 3 and 5) including the NPB derivative (entry 6) show completely reversible oxidation and the high HOMO levels that are close to the work function of ITO (−4.7 to −4.8 eV). It could be thus expected for **P3** to exhibit a facile hole-transporting property as observed in the polynorbornene-based HTL materials (entries 5 and 6) [27]. Despite the similar values, a slightly higher HOMO level of the naphthyl-containing homopolymer (**PNB Naph**) by *ca.* 0.05 eV than that of the copolymer (**P3**, 11.3 mol%) might be attributed to the increased electron density in the homopolymer owing to the presence of a large number of Lewis basic TAA groups.

4. Conclusion

We have demonstrated that the copolymerization of ethylene with 8-triarylamine substituted 1-octene monomers (**M1**–**M3**) efficiently leads to the triarylamine-functionalized polyethylene by use of various types of metallocene catalysts (**C1**–**C4**) in combination with MAO cocatalyst. These catalytic systems produced high-molecular-weight copolymers with controlled incorporation of comonomer although the sterically open catalyst (**C5**) suffered from Lewis acid–base interaction between the cationic metal center and the amine functionality, giving rise to poor catalytic performance. Analysis of copolymers having a moderate comonomer content (*ca.* 11 mol%, **P1**–**P3**) by NMR spectroscopy revealed well-defined polymer structure with the isolated comonomer units in the polymer chain. While UV–vis absorption and PL spectra of **P1**–**P3** suggest intrachain aggregate formation in solution particularly for phenyl and *m*-tolyl substituted triarylamine copolymers (**P1** and **P2**), high oxidational stability was observed for the **P2** and **P3** copolymers having *m*-tolyl and 1-naphthyl substituted triarylamines. The copolymers described here may hold promise as hole-transporting materials for optoelectronic device applications and relevant studies will be ongoing.

Acknowledgement

Financial supports from the Korea Science and Engineering Foundation (No. R01-2007-000-20299-0 for Y. Do) and the Priority Research Centers Program of the National Research Foundation of Korea (No. 2009-0093818 for M. H. Lee) are gratefully acknowledged. We would like to thank Honam Petrochemical Co. for help with the GPC analyses.

Appendix. Supplementary data

Supplementary data associated with this article can be found in the on-line version, at doi:10.1016/j.polymer.2010.08.033.

References

[1] Boaen NK, Hillmyer MA. Chem Soc Rev 2005;34(3):267–75.
[2] Yanjarappa MJ, Sivaram S. Prog Polym Sci 2002;27(7):1347–98.
[3] Naga N, Toyota A, Ogino K. J Polym Sci Part A Polym Chem 2005;43(4):911–5.
[4] Hakala K, Helaja T, Löfgren B. Polym Bull 2001;46(2):123–30.
[5] Wilén CE, Auer M, Strandén J, Näsman JH, Rotzinger B, Steinmann A, et al. Macromolecules 2000;33(14):5011–26.
[6] Mustonen I, Hukka T, Pakkanen T. Macromol Rapid Commun 2000;21 (18):1286–90.
[7] Stehling UM, Stein KM, Fischer D, Waymouth RM. Macromolecules 1999;32 (1):14–20.
[8] Stehling UM, Stein KM, Kesti MR, Waymouth RM. Macromolecules 1998;31 (7):2019–27.
[9] Stehling UM, Malmström EE, Waymouth RM, Hawker CJ. Macromolecules 1998;31(13):4396–8.
[10] Schneider MJ, Schäfer R, Mülhaupt R. Polymer 1997;38(10):2455–9.
[11] Kesti MR, Coates GW, Waymouth RM. J Am Chem Soc 1992;114(24):9679–80.
[12] Patil AO, Zushma S. Macromolecules 1998;31(6):1999–2001.
[13] Park MH, Huh JO, Do Y, Lee MH. J Polym Sci Part A Polym Chem 2008;46 (17):5816–25.
[14] Shirota Y, Kageyama H. Chem Rev 2007;107(4):953–1010.
[15] Bacher E, Bayerl M, Rudati P, Reckefuss N, Müller CD, Meerholz K, et al. Macromolecules 2005;38(5):1640–7.
[16] Snaith HJ, Whiting GL, Sun B, Greenham NC, Huck WTS, Friend RH. Nano Lett 2005;5(9):1653–7.
[17] Behl M, Hattemer E, Brehmer M, Zentel R. Macromol Chem Phys 2002;203 (3):503–10.
[18] Thelakkat M. Macromol Mater Eng 2002;287(7):442–61.
[19] Vasile C. Handbook of polyolefins. New York: Marcel Dekker; 2000.
[20] Sirringhaus H, Kawase T, Friend RH, Shimoda T, Inbasekaran M, Wu W, et al. Science 2000;290(5499):2123–6.
[21] Gustafsson G, Cao Y, Treacy GM, Klavetter F, Colaneri N, Heeger AJ. Nature 1992;357(6378):477–9.
[22] Cho J-Y, Domercq B, Barlow S, Suponitsky KY, Li J, Timofeeva TV, et al. Organometallics 2007;26(19):4816–29.
[23] Hreha RD, Haldi A, Domercq B, Barlow S, Kippelen B, Marder SR. Tetrahedron 2004;60(34):7169–76.
[24] Braunschweig H, Breitling FM. Coord Chem Rev 2006;250(21–22):2691–720.
[25] Gibson VC, Spitzmesser SK. Chem Rev 2003;103(1):283–316.
[26] Gladysz JA. Chem Rev 2000;100(4):1167–682.
[27] Park JH, Yun C, Park MH, Do Y, Yoo S, Lee MH. Macromolecules 2009;42 (18):6840–3.
[28] Razavi A, Ferrara J. J Organomet Chem 1992;435(3):299–310.
[29] Shapiro PJ, Cotter WD, Schaefer WP, Labinger JA, Bercaw JE. J Am Chem Soc 1994;116(11):4623–40.
[30] Stevens JC, Timmers FJ, Wilson DR, Schmidt GF, Nickias PN, Rosen RK, et al. Eur Pat Appl 0,416,815 A2; 1991.
[31] Canich JAM. US Pat 5,026,798; 1991.
[32] Hoye TR, Van Veidhuizen JJ, Vos TJ, Zhao P. Synth Commun 2001;31(9):1367–71.
[33] Bellmann E, Shaheen SE, Thayumanavan S, Barlow S, Grubbs RH, Marder SR, et al. Chem Mater 1998;10(6):1668–76.
[34] Koene BE, Loy DE, Thompson ME. Chem Mater 1998;10(8):2235–50.
[35] Liu W, Rinaldi PL, McIntosh LH, Quirk RP. Macromolecules 2001;34(14):4757–67.
[36] Randall JC. J Macromol Sci Rev Macromol Chem Phys 1989;C29(2&3):201–317.
[37] Melhuish WH. J Phys Chem 1961;65(2):229–35.
[38] Wang W-J, Kolodka E, Zhu S, Hamielec AE. J Polym Sci Part A Polym Chem 1999;37(15):2949–57.
[39] Suhm J, Schneider MJ, Mülhaupt R. J Mol Catal A Chem 1998;128 (1–3):215–27.
[40] Resconi L, Cavallo L, Fait A, Piemontesi F. Chem Rev 2000;100(4):1253–346.
[41] Adachi C, Tsutsui T, Saito S. Appl Phys Lett 1989;55(15):1489–91.
[42] Van Slyke SA, Chen CH, Tang CW. Appl Phys Lett 1996;69(15):2160–2.
[43] Lin BC, Cheng CP, Lao ZPM. J Phys Chem A 2003;107(26):5241–51.
[44] Stampor W, Mróz W. Chem Phys 2007;331(2–3):261–9.
[45] Lee CH, Ryu SH, Jang HD, Oh SY. Mater Sci Eng C 2004;24(1–2):87–90.
[46] Parab K, Venkatasubbaiah K, Jäkle F. J Am Chem Soc 2006;128(39):12879–85.
[47] Seo ET, Nelson RF, Fritsch JM, Marcoux LS, Leedy DW, Adams RN. J Am Chem Soc 1966;88(15):3498–503.
[48] D'Andrade BW, Datta S, Forrest SR, Djurovich P, Polikarpov E, Thompson ME. Org Electron 2005;6(1):11–20.